

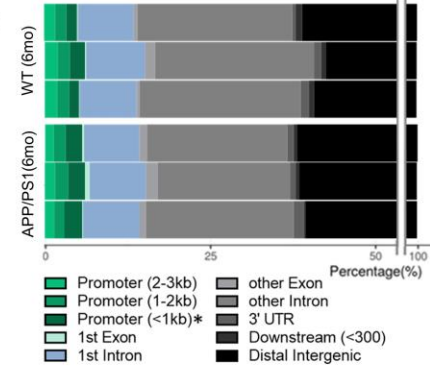
Supplementary Fig. 1 Expression level of MeCP2 in hippocampus and habenula showed no differences. (A, B) MeCP2 IHC staining of coronal sections including the striatal region of 6-mo WT and 6-mo APP/PS1 mice. IHC showed increased levels of MeCP2 expression in the dorsal striatum and the nucleus accumbens. Similar levels of MeCP2 signals found in comparing hippocampus and thalamus of WT and APP/PS1 mice. Scale bar: 800 μ m (C, D) IHC analysis of the MeCP2 expression level in coronal sections showing 3 subregions of the hippocampus; CA1, CA2 and DG. For lower panels, MeCP2 IHC images of medial habenula (mHb) and lateral habenula (lHb) in the epithalamic regions of WT and APP/PS1 mice are shown. Rectangles with dotted line indicate confocal microscopy magnified regions. Red scale bars: 200 μ m, white scale bars: 100 μ m, yellow scale bars: 40 μ m.

A

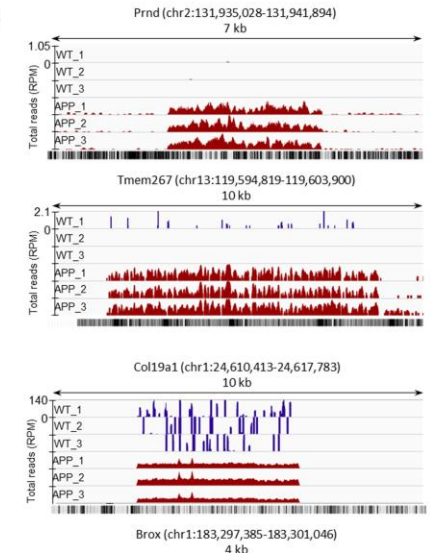
Group 2 704 gene symbol table

| Gene | Chr | Start | End | Symbol | Gene | Chr | Start | End | Symbol |
|---------------|---------------|----------------|--------------|---------|------------|------------|----------|---------|---------------|
| Aadat | Cdh18 | E03003006Rik | H2af1b1 | Malat1 | Olf1274-ps | Rbms3 | Tbct12b | Zfp600 | A130030018Rik |
| Aard | Cdh20 | E330013P04Rik | H2af1n | Mall1 | Olf1306 | Rbmy | Tbtf1r | Zfp746 | A430005M09Rik |
| Abca8b | Cdh9 | E3300161.19Rik | Hda | Mamld1 | Olf161 | Rex2 | Tbx20 | Zfp791 | A530032D15Rik |
| Abcb11 | Cdh8 | E330043G.19Rik | Hdcdos | Map2k6 | Olf248 | Rfx3 | Tbx22 | Zfp225 | A630008N07Rik |
| Abhd6 | Cdk5rap2 | Efd2r | Hexb | Map3k7 | Olf502 | Rfx3 | Tcp10c | Zfp445 | A830018L16Rik |
| Acacb | Cdk5rap2 | Edn1 | Hgsnat | Mast4 | Olf609 | Ric8b | Tcstv3 | Zfp495 | AA45190 |
| Adam21 | Cdk8 | Eea1 | Hic2 | Mbnl1 | Olf711 | Rnf217 | Tdr3 | Zfp981 | Gm10033 |
| Adcyap1 | Cdk8a | Efd2 | Hf1a | Mead9 | Olf696 | Robo2 | Tmem4 | Zfp982 | Gm10364 |
| Adgre5 | Cell2 | Efnas5 | Hnf4g | Meiv | Olf854 | Ror2 | Text1c1 | Zfp985 | Gm10649 |
| Adigr2 | Cenpf | Ei3 | Hnmpa112-ps2 | Mfnf9 | Ophn1 | Rp1 | Tex35 | Zfp987 | Gm10791 |
| Adigr3 | Cep350 | Elov5 | Hprt1 | Mir101c | Oabpl1a | Rplp1 | Tex47 | Zfp982 | Gm1110 |
| Aqab4 | Cept1 | Epha6 | Hpsa2 | Mir148a | Oxgr1 | Rps21 | Tfab2b | Znynd11 | Gm11217 |
| Ajap1 | Cerk | Epha7 | Hrasls | Mir205 | P3h2 | Rpr11 | Tec | Znh11 | Gm11487 |
| Albhd1a | Cfap54 | Epm2a | Hsba3 | Mir5127 | P4ha2 | Rpr2 | Tmem5 | Zplr1 | Gm12189 |
| Anot | Cfap59 | Erd1 | Hsbp1 | Mir5623 | Pabpc5 | Rps29 | Tlx27a | Zsr1 | Gm12887 |
| Ank1 | Chil5 | Esp24 | Hsd11b1 | Mir6236 | Pag1 | Rsp3a | Tia1 | Zwam6 | Gm13034 |
| Ankar | Ch1 | Esp38 | Hsfy2 | Mir6335 | Pak3 | Rsp3b | Tiam2 | Zwit | Gm13212 |
| Ankle1 | Chst11 | Esr1 | Htra3 | Mir6336 | Pan3 | Sall1 | Tmem21 | | Gm13238 |
| Anx2 | Chd2 | Cz3b | Icf1 | Mir6356 | Pcdh15 | Scq3 | Tlet | | Gm13580 |
| Ano5 | Chd34d | Fam107a | Ilna13 | Mir6370 | Pcdh18 | Schp1 | Tle4 | | Gm13710 |
| Appb1ip | Cntn5 | Fam171a1 | Ilnk3 | Mir6393 | Pcdh7 | Sak2 | Tmem114 | | Gm14296 |
| App | Cntnag2 | Fam172a | Irg2b | Mir6965 | Polo | Sarpanb9f | Tmem125 | | Gm14486 |
| Arhgap21 | Cntnaps5a | Fam174a | Ighmbp2 | Mir704 | Pcnx2 | Satd4 | Tmem18 | | Gm14525 |
| Arhgap26 | Cntnaps5c | Fam213b | Iikzf2 | Mir7211 | Pde1c | Sgk3 | Tmem196 | | Gm14632 |
| Arhgap28 | Col1 | Fam33a | Ilttrap1 | Mir7224 | Pept | Siglech | Tmem267 | | Gm14851 |
| Arhgap28 | Col11a1 | Farp1 | Irl1a | Mir7105 | Pea2 | Sirt1 | Tmem56 | | Gm15246 |
| Arnt | Col19a1 | Fbxo33 | Incpn | Mixc | PHF21a | Skint6 | Tmx3 | | Gm15679 |
| Arndc3 | Col4a6 | Fbxw4 | Inpp4b | Mogat1 | Phx4 | Sic15a2 | Tmx4 | | Gm16551 |
| Aant | Col6a6 | Fbxw7 | Inpp5f | Mirgag4 | Pik6 | Sic16a14 | Tnks | | Gm16973 |
| Arz | Cope1 | Ferb5 | Irfk | Mragap2 | Pik6 | Sic16a9 | Tnfr2 | | Gm17019 |
| Atg4c | Cp | Fgf12 | Ijw | Mrlp3 | Pisid-ps1 | Sic22a12 | Tnfrs60 | | Gm17644 |
| Atp5g1 | Cpeb2 | Fgf14 | Iqcm | Mrf4a | Pisid-ps2 | Sic24a3 | Tnfrk | | Gm17660 |
| Cp1 | Cp1 | Fgln | Iat1 | Maz2 | Sic20a4 | Tnfrp1 | Tnfr1 | | Gm19689 |
| AW20091 | Cpccr1 | Filip1 | Iga1 | Msl3l2 | Pikx2 | Sic39a10 | Tslp | | Gm19782 |
| Axin2 | Cr2 | Fmn1 | Ilgal1 | Mtpap | Pknox1 | Sic61a11 | Tspan3 | | Gm1993 |
| B230118H07Rik | Creb3l1 | Fndc1 | Ilgap9 | Mtrr | Plag2l2b | Silkr1 | Tnfr1 | | Gm20063 |
| B230307C23Rik | Creb3l1 | Fmxd | Irfk | Muc8 | Silkr5 | Tnfrs11 | Tnfrs11 | | Gm20088 |
| B2galn2 | Crp | Frmf4a | Iltn1 | Mug-ps1 | Picb4 | Smarca5-ps | Tyrp1 | | Gm20352 |
| Bambi | Caf2ra | Frmf4b | Jam3 | Mydgf | Picb4 | Smarca5-ps | Tyrp1 | | Gm20554 |
| Bat3 | Csk | Frmf4f | Jarid2 | Myf12b | Pis2 | Sme5 | Ublf11 | | Gm20594 |
| Bbox1 | Csm3d3 | Frmf4f | Kcnk22 | Mylo | Plekha1 | Smin101 | Uchl5 | | Gm20594 |
| BC048403 | Cyp2b19 | Fscb | Kcnh13 | Myo7a | Pirg1 | Smin13 | Utr1 | | Gm20740 |
| Bmgrp1b | Cyp2c40 | G5300110D6Rik | Kcnh5 | Myom2 | Pisdc2 | Smo | Unc5d | | Gm20752 |
| Bmgrp3 | Cyp2c50 | G53005G22Rik | Kcnk1 | Myo7b | Pisdc1 | Sma | Upp2 | | Gm20755 |
| Brox | Cyp2c66 | Glabp2 | Kcnip4 | Nalc | Podal | Nalc | Upp2 | | Gm20826 |
| Btd35f12 | Cyp2c69 | Gad2 | Kcnk2 | Nampt | Pok3k | Snrpe | Vmn1r238 | | Gm20939 |
| Btd35f27 | Cyp4a12b | Galm5 | Kcnm2 | Nba | Pou4f1 | Sno | Vmn1r60 | | Gm21083 |
| Btd35f28 | Cyp4a12b | Galm5 | Kcnm2 | Nba | Pou4f1 | Sno | Vmn1r60 | | Gm21083 |
| C13002621Rik | Cypr1 | Gfra1 | Kctd16 | Nectin3 | Ppp1r9a | Sp110 | Vmn2r102 | | Gm21190 |
| C230029F24Rik | D030025E07Rik | Ggh | Khdcb1b | Nesd4l | Ppp2r2b | Sgap17 | Vmn2r114 | | Gm21379 |
| C230011F03Rik | D030045P18Rik | Ghr1 | Klf5 | Nesl10 | Ppp4r2 | Spear4e | Vmn2r120 | | Gm21814 |
| Cadps | D13000918Rik | Gnb1l | Kilhd4 | Nemf | Ppp6c | Spear4cos | Vmn2r29 | | Gm22669 |
| Camsap2 | D430019H16Rik | Gng4 | Klhl4 | Neto1 | Prpp | Spear4e | Vmn2r72 | | Gm24981 |
| Cagrn | D5Erd579e | Gnp2a2 | Kirb1b | Nfasc | Prex2 | Spear4f1 | Vmn2r77 | | Gm25896 |
| Car15 | Dakp1 | Gphn | Kpna1 | Nkx2 | Prde | Spear5-ps1 | Vmn2r97 | | Gm26251 |
| Carpt | Dhdh1 | Gpm6a | Ktn1 | Nkain3 | Prnd | Spear5-ps1 | Vps45 | | Gm26598 |
| Catsperb | Ddx18 | Gpr12 | Lama1 | Nkx2-6 | Prnp | Sspn | Waf3 | | Gm38397 |
| Ch3 | Dlga2 | Gpr151 | Large1 | Nobox | Prps1 | Sxab6 | Wdr19 | | Gm4305 |
| Cdc33 | Dmd | Gpr12 | Lbr | Nesl1 | Pich3 | Sgap1 | Wfs | | Gm4710 |
| Cdc373 | Dnrt11 | Gram33 | Lhfp2 | Nova1 | Ptger3 | Ston1 | Wnt16 | | Gm4850 |
| Cdc50b | Dnahe6 | Greb1 | Limd1 | Nrn1 | Ptprn2 | Sixb4 | Wwox | | Gm4981 |
| Cgmp2 | Dnahe7b | Gria1 | Lipr2 | Ptprn | Ptprn | Sixb5 | Xcr1 | | Gm5470 |
| Ccnh | Dock2 | Grid2 | Litaf | Nfse | Pthrt1 | Suit2a1 | Yba3 | | Gm5458 |
| Ccr1 | Dok4 | Grin3a | Lmbrd1 | Ntrk3 | Rab10os | Sympk | Ythdf3 | | Gm5935 |
| Ccl180 | Dpp10 | Grp | LOC100861615 | Nuph1 | Rab39b | Tab2 | Zdhbc3 | | Gm6194 |
| Ccl208a | Dyr18l1 | Gria2 | Lrrc4c | Nysr1 | Rac3l1 | Tar2114 | Zfp125 | | Gm6760 |
| Ccl300c | Drd2 | Gzfrd1 | Lrrn1 | Oas1 | Rap2b | Tasr115 | Zfp389 | | Gm7102 |
| Ccl44 | Drosha | Gtpbp4 | Lrrn3 | Olfm4 | Rarb | Tbctd14 | Zfp468 | | Gm7134 |
| Cdhl1 | Dyr18l1 | Gria2 | Lrrc4c | Olf1189 | Rasab9 | Tbctd22a | Zfp534 | | Gm7827 |
| Cdhl2 | Dyhn | Gutp1 | Mageb18 | Olf1200 | Rbfox1 | Tbctd23 | Zfp598 | | Gm7877 |

B



C



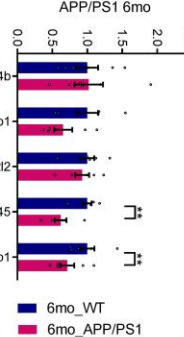
D

Gene ontology analysis for Groups2 704 genes

| Category | Term | P-Value | Fold Enrichment |
|------------------|--|---------|-----------------|
| KEGG_PATHWAY | mmu05030 Cocaine addiction | 0.039 | 3.989 |
| KEGG_PATHWAY | mmu00590 Arachidonic acid metabolism | 0.002 | 3.831 |
| KEGG_PATHWAY | mmu04512 ECM-receptor interaction | 0.008 | 3.444 |
| KEGG_PATHWAY | mmu05204 Chemical carcinogenesis | 0.010 | 3.294 |
| KEGG_PATHWAY | mmu04360 Axon guidance | 0.020 | 2.643 |
| GOTERM_BP_DIRECT | GO:0021756-stratum development | 0.005 | 10.969 |
| GOTERM_BP_DIRECT | GO:0035810-positive regulation of urine volume | 0.005 | 10.969 |
| GOTERM_BP_DIRECT | GO:0042129-regulation of T cell proliferation | 0.032 | 10.470 |
| GOTERM_BP_DIRECT | GO:1901379-regulation of potassium ion transmembrane transport | 0.006 | 10.238 |
| GOTERM_BP_DIRECT | GO:0060134-prepulse inhibition | 0.006 | 10.238 |
| GOTERM_MF_DIRECT | GO:0004609-phosphatidyserine decarboxylase activity | 0.100 | 19.256 |
| GOTERM_MF_DIRECT | GO:0004708-MAP kinase kinase activity | 0.021 | 12.837 |
| GOTERM_MF_DIRECT | GO:0004435-phosphatidylinositol phospholipase C activity | 0.009 | 9.062 |
| GOTERM_MF_DIRECT | GO:0030676-Rac guanyl-nucleotide exchange factor activity | 0.050 | 8.253 |
| GOTERM_MF_DIRECT | GO:0004620-phospholipase activity | 0.056 | 7.702 |
| GOTERM_CC_DIRECT | GO:1990761-growth cone lamellipodium | 0.077 | 25.256 |
| GOTERM_CC_DIRECT | GO:0034705-potassium channel complex | 0.033 | 10.332 |
| GOTERM_CC_DIRECT | GO:0060077-inhibitory synapse | 0.002 | 9.020 |
| GOTERM_CC_DIRECT | GO:0030673-axolemma | 0.013 | 7.976 |
| GOTERM_CC_DIRECT | GO:0044291-cell-cell contact zone | 0.073 | 6.685 |

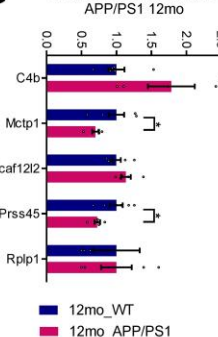
F

Fold change target mRNA APP/PS1 6mo



G

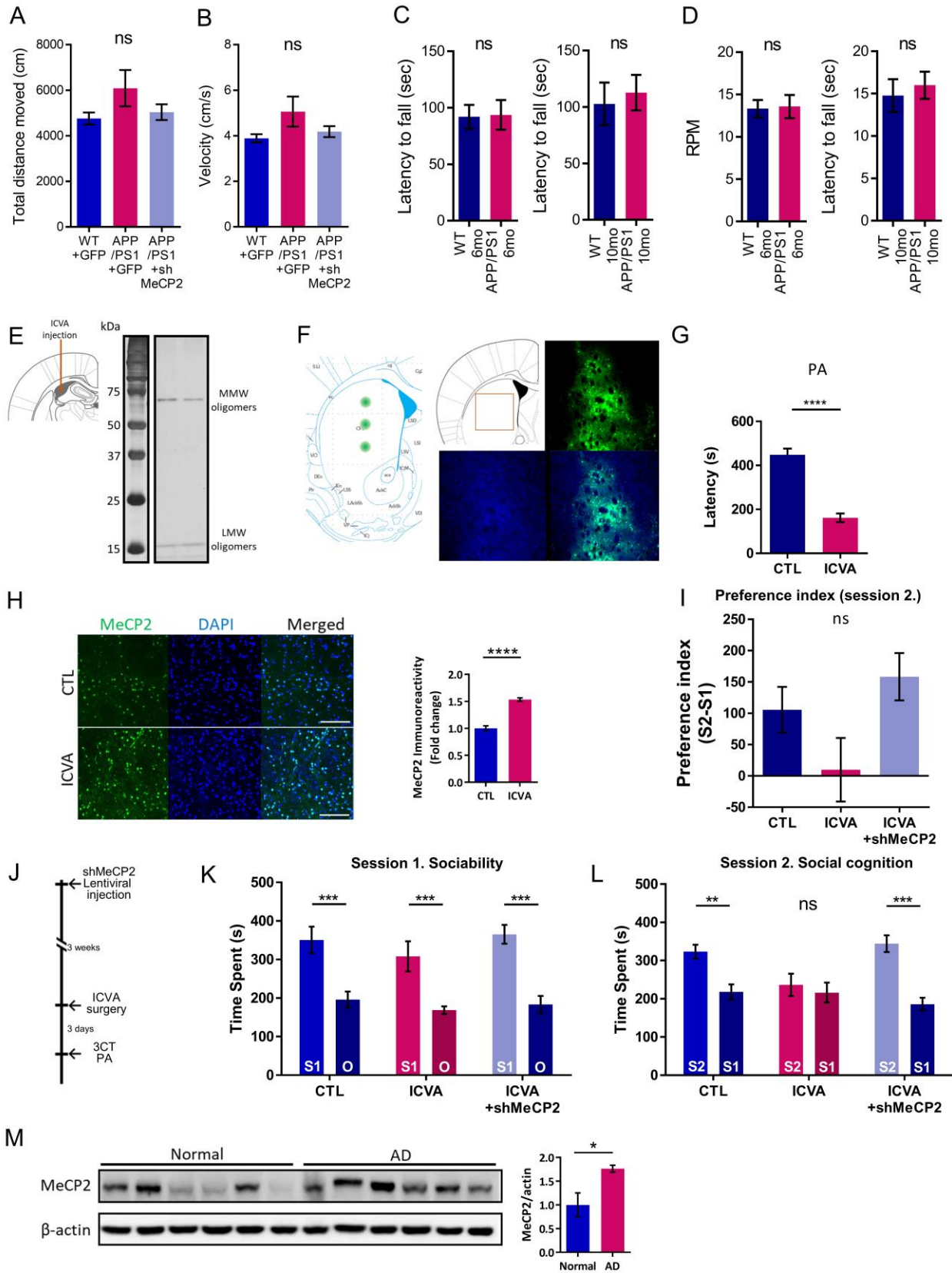
Fold change target mRNA APP/PS1 12mo



H

| Gene | Ref. | Neuronal function |
|----------|---------------------------------|---|
| C4b | <i>Mol Psychiatry</i> (2021) | Protective effect of complement component 4 (C4A, C4B) and HSPA2 to the APOE ε2 in Alzheimer disease |
| | <i>J Neurochem</i> (2015, 2016) | Calcium sensor for the baseline neurotransmitter release and for the induction and long-term maintenance of presynaptic homeostatic plasticity. |
| Dcaf12l2 | - | - |
| Prss45 | - | - |
| Rplp1 | <i>PLoS One</i> (2014) | Ribosomal protein for embryonic development of the nervous system |
| | <i>Mol Brain</i> (2021) | - |

Supplementary Fig. 2 MeCP2-ChIP-seq analysis revealed various biological pathways which were altered by dysregulated binding of MeCP2. (A) Table of the 704 target genes of which promoter regions were heavily occupied by MeCP2 in the APP/PS1 mice compared with the WT group. (B) Divided bar charts of individual samples showing the coverage of MeCP2 bound regions of the WT and APP/PS1 groups (WT n = 3; APP/PS1 n = 3). Colored boxes indicate corresponding binding regions on the bar chart. (C) Representative binding pattern images of IGV analysis showing de-novo binding patterns of the accumulated read count peaks of the ChIPed-DNA fragments from selected regions. Green bars indicate the CpG island regions detected in the UCSC genome browser. (D) Via DAVID functional annotation bioinformatics analysis, KEGG pathways and GO terms of group2 genes turned out to be involved in multiple biological pathways associated with neurodegenerative diseases. (E) ChIP-qPCR analysis of selected target regions using MeCP2-ChIPed genomic DNA. Experimental control of ChIP reaction was labelled as IP- and results were presented in percentage of total input amount (IP- n = 3; MeCP2-IP n = 3; unpaired *t*-test, **P* < 0.05, ***P* < 0.01, ****P* < 0.001). (F-G) RT-qPCR analysis of selected target genes from RNA sample of striatum of 6-month and 12-month old mice (for each WT n = 6; APP/PS1 n = 6; unpaired *t*-test, **P* < 0.05, ***P* < 0.01). (H) Reported function of the selected target genes in relation to AD and other functions in the brain.



Supplementary Fig. 3 ICVA mouse showed impaired behaviors in the social novelty seeking. (A) Total distance moved during Session 1 and Session 2 of 3CT. (B) Velocity of movement during 3CT (for (A) and (B), mean \pm SEM, WT+GFP n = 6; APP/PS1+GFP n = 3; APP/PS1+shMeCP2 n = 8, ns: not significant). (C) Latency to fall in the RTT of APP/PS1 and WT mice. (D) RPM to fall from the accelerating rotarod (for (C) and (D), mean \pm SEM, (6-mo WT n = 9; 6-mo APP/PS1 n = 8; 10-mo WT n = 3; 10-mo APP/PS1 n = 6, ns: not significant). (E) Illustration of brain coronal sections representing the target location of ICV injection of A β ₁₋₄₂, and silver staining of A β ₁₋₄₂ solution prepared for ICV injection showed two bands of MMW (middle molecular weight) oligomers and LMW (low molecular weight) oligomers. (F) Virus-injected tissue showed widespread expression of GFP from the injection site throughout the entire striatum. (G) PA test of ICVA mice and vehicle control. The time elapsed to escape the dark chamber is shown as latency in seconds (CTL n = 10; ICVA n = 12; unpaired *t*-test, *****P* < 0.0001). (H) MeCP2 IHC (green) and DAPI (blue) staining of the striatum in ICVA mice. Scale bars: 100 μ m. Signal intensity of MeCP2 immunoreactivity was quantified and displayed as fold change in MeCP2 immunoreactivity (CTL n = 4; ICVA n = 4; unpaired *t*-test, *****P* < 0.0001) (I) Preference index of the second session of the 3CT, as the difference in total time spent in the S2 chamber as to the S1 chamber for CTRL, ICVA, and ICVA+shMeCP2 mice (CTL n = 4; ICVA n = 6; ICVA+shMeCP2 n = 8, ns: not significant). (J) Experimental schedule of behavioral tests after the stereotaxic injection of shMeCP2 virus. Behavioral tests were conducted 3 weeks after the surgery and 3 days after the ICVA treatment. (K) Time spent in chambers shown as a measure of sociability in the first session of the 3CT for CTL, ICVA, and ICVA+shMeCP2 groups (CTL n = 4; ICVA n = 6; ICVA+shMeCP2 n = 8; unpaired *t*-test, ***P* < 0.01, ****P* < 0.001). (L) Time spent in chambers as a measure of novelty-seeking in the second session of 3CT for CTL, ICVA, and ICVA+shMeCP2 groups (CTL n = 4; ICVA n = 6; ICVA+shMeCP2 n = 8; unpaired *t*-test, ***P* < 0.01, ****P* < 0.001). (M) Increased MeCP2 levels in the postmortem forebrain regions of AD patients. MeCP2 protein levels in the postmortem forebrain region of the brain from AD patients compared to the brains from healthy controls (Normal). Western blot analysis and the following densitometry calculation (Normal n = 6; AD n = 6; unpaired *t*-test, **P* < 0.05).

Supplementary Table 1. Information of postmortem brain tissue samples from normal subjects and AD patients.

| Number | Diagnosis/Case | Age | Sex | Braak stage |
|--------|----------------|-----|--------|-------------|
| 1 | Normal | 87 | Female | I |
| 2 | Normal | 88 | Male | I |
| 3 | Normal | 86 | Male | II |
| 4 | Normal | 87 | Female | II |
| 5 | Normal | 82 | Male | I |
| 6 | Normal | 82 | Male | I |
| 1 | AD | 85 | Male | V |
| 2 | AD | 87 | Female | V |
| 3 | AD | 82 | Male | V |
| 4 | AD | 80 | Female | V |
| 5 | AD | 83 | Male | VI |
| 6 | AD | 89 | Male | IV |